

# On the nonlinear axisymmetric dynamic buckling behavior of clamped functionally graded spherical caps

T. Prakash<sup>a</sup>, N. Sundararajan<sup>b</sup>, M. Ganapathi<sup>c,\*</sup>

<sup>a</sup>*Department of Applied Mechanics, Indian Institute of Technology Delhi, New Delhi 110016, India*

<sup>b</sup>*Department of Mechanical Engineering, The University of Akron, Akron, OH, USA*

<sup>c</sup>*Institute of Armament Technology, Girinagar, Pune 4110 025, India*

Received 11 March 2005; received in revised form 19 June 2006; accepted 23 June 2006

Available online 25 September 2006

---

## Abstract

Here, the dynamic thermal buckling behavior of functionally graded spherical caps is studied considering geometric nonlinearity based on von Karman's assumptions. The formulation is based on first-order shear deformation theory and it includes the in-plane and rotary inertia effects. The material properties are graded in the thickness direction according to the power-law distribution in terms of volume fractions of the material constituents. The effective material properties are evaluated using homogenization method. The governing equations obtained using finite element approach are solved employing the Newmark's integration technique coupled with a modified Newton–Raphson iteration scheme. The pressure load corresponding to a sudden jump in the maximum average displacement in the time history of the shell structure is taken as the dynamic buckling load. The present model is validated against the available isotropic case. A detailed numerical study is carried out to highlight the influences of shell geometries, power law index of functional graded material and boundary conditions on the dynamic buckling load of shallow spherical shells.

© 2006 Elsevier Ltd. All rights reserved.

---

## 1. Introduction

Thin spherical shells form an important class of structural components, with many significant applications in engineering fields. The dynamic response of such shells may lead to the phenomenon of dynamic snapping or dynamic buckling. As these kinds of responses cannot be evaluated accurately using small displacement theory, studies based on nonlinear dynamic analysis has received considerable attention in the literature.

The analysis of isotropic shallow spherical shells has been carried out by Budiansky and Roth [1], Simitses [2], Haung [3], Stephens and Fulton [4], Ball and Burt [5], and Stricklin and Martinez [6]. Budiansky and Roth [1] have employed the Galerkin method whereas Simitses [2], adopted Ritz-Galerkin procedure. A finite difference scheme has been introduced in the method of solution by Haung [3], Stephens and Fulton [4], Ball and Burt [5], and Kao [6] while Stricklin and Martinez [7], Saigal et al. [8] and Yang and Liaw [9] utilized

---

\*Corresponding author. No. 925 Scientist Hostel III, DRDO Township: Phase I, C.V. Raman Nagar (PO) Bangalore 560093, India. Tel.: +91 80 25240265.

E-mail address: [mganapathi@rediffmail.com](mailto:mganapathi@rediffmail.com) (M. Ganapathi).

efficient finite element procedure. The limited studies available on axisymmetric dynamic buckling of single-layer orthotropic shallow spherical shells are based on classical lamination theory [10,11], and multilayered case by Ganapathi et al. [12].

The use of functionally graded materials as structural components has gained much popularity in recent years. Functionally graded materials are composite materials that are microscopically inhomogeneous, and the mechanical properties vary smoothly or continuously from one surface to the other. It is this continuous change that results in gradient properties in functionally graded materials. Typically, these materials are made from a mixture of ceramic and metal, or a combination of different materials. The concept of functionally graded materials (FGMs) was first introduced in 1984 by the group of material scientists in Japan, as ultrahigh temperature resistant materials for aircraft, space vehicles and other engineering applications [13]. Studies in FGM structures are largely confined to the analysis of thermal stress and deformation [14–16]. Analytical and numerical studies have been carried out to investigate the thermo-mechanical behavior of FGMs [17–19]. Due to non-homogeneous nature of FGM and the high mathematical complexities involved, only few investigations on transient dynamic responses of FGM are yet known in the literature [20–23]. The vibration and parametric instability analysis of functionally graded cylindrical shells under harmonic axial loading has been studied in Refs. [24,25]. However, to the authors’ knowledge, work on the axisymmetric dynamic buckling behavior of functionally graded material spherical shells is not commonly available in the literature, and such study is immensely useful to the designers while optimizing the designs of FGMs structures under dynamic situation.

Here, a three-noded shear flexible axisymmetric curved shell element developed based on the field-consistency principle [12,26] is employed to analyze the axisymmetric dynamic buckling of clamped functionally graded spherical caps under externally applied pressure load. Geometric nonlinearity is assumed in the present study using von Karman’s strain–displacement relations. The material properties are graded in the thickness direction according to the power-law distribution in terms of volume fractions of the constituents of the material. The nonlinear governing equations derived are solved employing direct integration method. The dynamic buckling pressure is taken as the pressure corresponding to a sudden jump in the maximum average displacement in the time history of the shell structure [1,27]. Numerical results are presented considering different values for geometrical parameter, and power law index on the dynamic bucking behavior of functionally graded spherical caps.

## 2. Theoretical formulation

An axisymmetric functionally graded shell of revolution with radius  $a$ , thickness  $h$  made of a mixture of ceramics and metals is considered with the coordinates  $s$ ,  $\theta$  and  $z$  along the meridional, circumferential and radial/thickness directions, respectively, as shown in Fig. 1. The materials in outer ( $z = h/2$ ) and inner ( $z = -h/2$ ) surfaces of the shell are ceramic and metal, respectively. The Young’s modulus  $E$  and density  $\rho$  can be determined based on Voigt’s rule over the whole range of the volume fraction [28] as

$$E(z) = E_c V_c + E_m(1 - V_c), \quad \rho(z) = (\rho_c V_c - \rho_m(1 - V_m)), \quad (1)$$

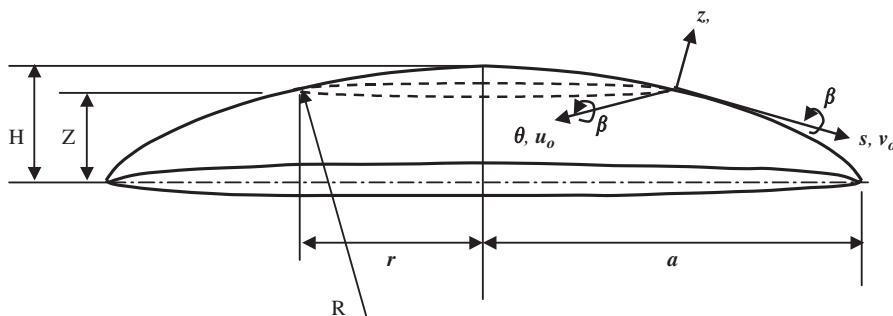


Fig. 1. Geometry and the coordinate system of a spherical cap.

where  $V_c$  is the volume fractions of ceramic and is assumed as a power function [29] as

$$V_c(z) = \left( \frac{2z+h}{2h} \right)^k. \quad (2)$$

Here,  $k$  refers the volume fraction exponent ( $k \geq 0$ ) and Poisson's ratio  $\nu$  is assumed to be constant. The variation of the composition of ceramic and metal is linear for  $k = 1$ . The value of  $k$  equal to zero represents a fully ceramic shell.

By using the Mindlin formulation, the displacements at a point  $(s, \theta, z)$  are expressed as functions of the mid-plane displacements  $u_0, v_0$  and  $w$ , and independent rotations  $\beta_s$  and  $\beta_\theta$  of the radial and hoop sections, respectively, as

$$\begin{aligned} u(s, \theta, z, t) &= u_0(s, \theta, t) + z\beta_s(s, \theta, t), \\ v(s, \theta, z, t) &= v_0(s, \theta, t) + z\beta_\theta(s, \theta, t), \\ w(s, \theta, z, t) &= w(s, \theta, t), \end{aligned} \quad (3)$$

where  $t$  is the time.

Using von Karman's assumption for moderately large deformation, Green's strains can be written in terms of middle-surface deformations as

$$\{\varepsilon\} = \left\{ \begin{matrix} \varepsilon_p^L \\ 0 \end{matrix} \right\} + \left\{ \begin{matrix} z\varepsilon_b \\ \varepsilon_s \end{matrix} \right\} + \left\{ \begin{matrix} \varepsilon_p^{NL} \\ 0 \end{matrix} \right\} \quad (4)$$

where, the membrane strains  $\{\varepsilon_p^L\}$ , bending strains  $\{\varepsilon_b\}$ , shear strains  $\{\varepsilon_s\}$  and nonlinear in-plane strains  $\{\varepsilon_p^{NL}\}$  in the Eq. (4) are written as [30]

$$\begin{aligned} \left\{ \varepsilon_p^L \right\} &= \left\{ \begin{matrix} \frac{\partial u_0}{\partial s} + \frac{w}{R} \\ \frac{u_0 \sin \phi}{r} + \frac{w \cos \phi}{r} \\ -\frac{v_0 \sin \phi}{r} + \frac{\partial v_0}{\partial s} \end{matrix} \right\}, & \left\{ \varepsilon_b \right\} &= \left\{ \begin{matrix} \frac{\partial \beta_s}{\partial s} + \frac{\partial u_0}{R \partial s} \\ \frac{\beta_s \sin \phi}{r} + \frac{u_0 \sin \phi}{Rr} \\ \frac{\partial v_0 \cos \phi}{\partial s} + \frac{\partial \beta_\theta}{\partial s} - \frac{\beta_\theta \sin \phi}{r} \end{matrix} \right\}, \\ \left\{ \varepsilon_s \right\} &= \left\{ \begin{matrix} \beta_s + \frac{\partial w}{\partial s} \\ \beta_\theta - \frac{v_0 \cos \phi}{r} \end{matrix} \right\}, & \left\{ \varepsilon_p^{NL} \right\} &= \left\{ \begin{matrix} \frac{1}{2} \left( \frac{\partial w}{\partial s} \right)^2 \\ 0 \\ 0 \end{matrix} \right\}, \end{aligned}$$

where  $r, R$  and  $\phi$  are the radius of the parallel circle, radius of the meridional circle and angle made by the tangent at any point in the middle-surface of the shell with the axis of revolution.

The potential energy functional  $U$  can be written in terms of the field variables  $u_0, v_0, w, \beta_s, \beta_\theta$  and their derivatives, following the procedure given in the work of Rajasekaran et al. [31], as

$$U(\delta) = \{\delta\}^T [(1/2)[K] + [(1/6)[N_1(\delta)] + (1/12)[N_2(\delta)]]\{\delta\} + \{\delta\}^T \{F\}, \quad (5)$$

where  $[K]$  is the linear stiffness matrix  $[N_1]$  and  $[N_2]$  are the nonlinear stiffness matrices linearly and quadratically dependent on the field variables, respectively, and  $\{F\}$  is the load vector due to externally applied pressure load.  $\{\delta\}$  is the vector of the degree of freedom associated to the displacement field in a finite element discretization.

The kinetic energy of the shell is given by

$$T(\delta) = (1/2) \int_A [p(\dot{u}_0^2 + \dot{v}_0^2 + \dot{w}_0^2) + I(\dot{\beta}_s^2 + \dot{\beta}_\theta^2)] dA, \quad (6)$$

where

$$p = \int_{-h/2}^{h/2} \rho(z) dz, \quad I = \int_{-h/2}^{h/2} z^2 \rho(z) dz$$

and  $\rho(z)$  is the mass density which varies through the thickness of the shell and is given by Eq. (1). The dot over the variable denotes derivative with respect to time. Using Eqs. (5) and (6) in Lagrange's equation of motion, the governing equation for the shell is obtained as

$$[M]\{\ddot{\delta}\} + [[K] + \frac{1}{2}[N_1(\delta)] + \frac{1}{3}[N_2(\delta)]]\{\delta\} = \{F\}, \quad (7)$$

where  $[M]$  is the mass matrix.

The nonlinear equation (7) is solved by the Newmark's numerical integration method [32]. Equilibrium is achieved for each time step through modified Newton–Raphson iteration until the convergence criteria [33] are satisfied within the specific tolerance limit of less than one percent. The dynamic buckling loads are evaluated based on the displacement response obtained from Eq. (7).

The criterion suggested by Budiansky and Roth [1] is employed here as it is widely accepted. This criterion is based on the plots of the peak non-dimensional average displacement in the time history of the structure with respect to the amplitude of the pressure load (e.g. inserted figure in Fig. 3). There is a load range where a sharp jump in peak average displacement occurs for a small change in load magnitude. The inflection point of the load–deflection curve is considered as the dynamic buckling load.

### 3. Results and discussion

In this section, we use the above formulation to investigate the effect of parameters such as material power law index and geometric shell parameter on the dynamic buckling pressure of clamped functionally graded spherical caps subjected to externally applied pressure load. Since the finite element used here is based on the field consistency approach, an exact integration is employed to evaluate all the strain energy terms. The shear correction factor, which is required in a first-order theory to account for the variation of transverse shear stresses, is taken as 5/6. For the present analysis, based on progressive mesh refinement, 15-element idealization is found to be adequate in modeling the spherical caps. The performance of the element has been dealt in Refs. [12,26]. For the sake of brevity, such study is not shown here. The initial conditions for obtaining the nonlinear dynamic response are assumed as zero values for the displacements and velocities. From the dynamic response curves, the load amplitudes and the corresponding maximum average displacements are obtained for applying the buckling criteria. The constants  $\alpha$  and  $\beta$  (controlling parameters for stability and accuracy of the solution) in the Newmark's integration are taken as 0.5 and 0.25, which correspond to the unconditionally stable scheme in the linear analysis. Since there is no estimate of the time step for the nonlinear dynamic analysis available in the literature, the critical time step of a conditionally stable finite difference scheme [34] is introduced as a guide and a convergence study was conducted to select a time step which yields a stable and accurate solution.

Fig. 2 shows the variations of the volume fractions of ceramic and the stiffness/Young's modulus in the thickness direction  $z$  for the FGM spherical cap. The outer surface is ceramic rich and the inner surface is metal rich. The FGM spherical shell considered here consists of aluminum (Al) and alumina ( $Al_2O_3$ ). The Young's modulus, conductivity and the coefficient of thermal expansion for alumina is  $E_c = 380$  GPa,  $\kappa_c = 10.4$  W/mK,  $\alpha_c = 7.4 \times 10^{-6}$   $1/^\circ\text{C}$ , and for aluminum is  $E_m = 70$  GPa,  $\kappa_m = 204$  W/mK,  $\alpha_m = 23 \times 10^{-6}$   $1/^\circ\text{C}$ , respectively. Poisson's ratio is chosen as constant,  $\nu = 0.3$ . The spherical cap is of uniform thickness and clamped boundary conditions considered here is

$$u_0 = v_0 = w = \beta_s = \beta_\theta = 0 \quad \text{on } r = a.$$

Results of non-dimensional dynamic pressure,  $P_{cr}$ , are presented for functionally graded spherical caps for different values of the geometrical parameter  $\lambda$ .  $P_{cr}$  and  $\lambda$  are defined as

$$P_{cr} = \frac{1}{8}[3(1 - \nu^2)]^{1/2} \left(\frac{h}{H}\right)^2 \frac{qa^4}{E_c h^4}, \quad \lambda = 2[3(1 - \nu^2)]^{1/4} \left(\frac{H}{h}\right)^{1/2}.$$

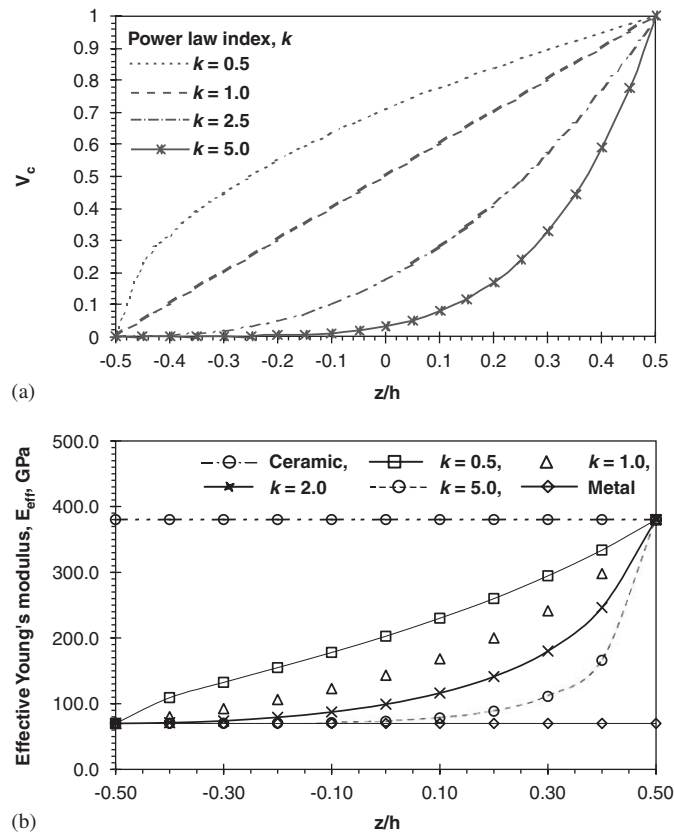


Fig. 2. Variation of (a) volume fraction of ceramic; and (b) Young's modulus through thickness of FGM spherical shell.

Here,  $H$  and  $a$  are the central shell rise and base radius, respectively. For the chosen shell parameter and power law index of FGM, the dynamic buckling study is firstly conducted for step loading of infinite duration. The length of response calculation time  $\tau$  ( $= \sqrt{(E_{\text{ef}} h^2 / 12(1 - \nu^2) \rho_{\text{ef}} a^4) t}$ ) in the present study is varied between 1 and 2 with the criterion that in the neighborhood of the buckling,  $\tau$  is large enough to allow deflection–time curves to develop fully.  $E_{\text{ef}} (= (1/2) \int_{-h/2}^{h/2} E(z) dz)$ , and  $\rho_{\text{ef}} (= (1/2) \int_{-h/2}^{h/2} \rho(z) dz)$  correspond to effective modulus and density of FGM for the chosen gradient index, respectively. The time step selected, based on the convergence study, is  $\delta\tau = 0.002$ . The value selected for  $\tau$  and  $\delta\tau$  is of the same order as that of Refs. [5,7].

Fig. 3 highlights the typical nonlinear axisymmetric dynamic response history with time for the functionally graded spherical shell parameter ( $\lambda = 6$ ,  $a/h = 400$  and  $k = 1.0$ ), considering different externally applied pressure loads. Further, using such plots, the variation of maximum average displacement with applied load obtained is also highlighted as an inset in Fig. 3 for predicting the critical load. It is seen that there is a sudden jump in the value of the average displacement when the external pressure reaches the value  $P_{\text{cr}} = 0.6063$  for the shell considered here. The dynamic snap-through loads predicted in this manner for different values material power law index are presented in Fig. 4. For comparison purpose, the available analytical results [3] for isotropic case are also shown in Fig. 4. It is seen that the present results for pure ceramic case ( $k = 0$ ) are found to be in very good agreement. However, while comparing with those of Ref. [12] for the isotropic case (not shown here), some differences for the deep shell parameter may be noticed due to different maximum time length  $\tau$  employed for shallow and deep cases. Here,  $\tau$  is limited to around 2.5, irrespective of type of shells whereas it is about 2 in Ref. [12] for deep shell case. Furthermore, it is revealed from Fig. 4 that, with the increase in power law index  $k$ , the critical buckling pressure decreases, irrespective of shell geometrical parameter. This is attributed possibly due to the stiffness degradation occurs because of the increase in the

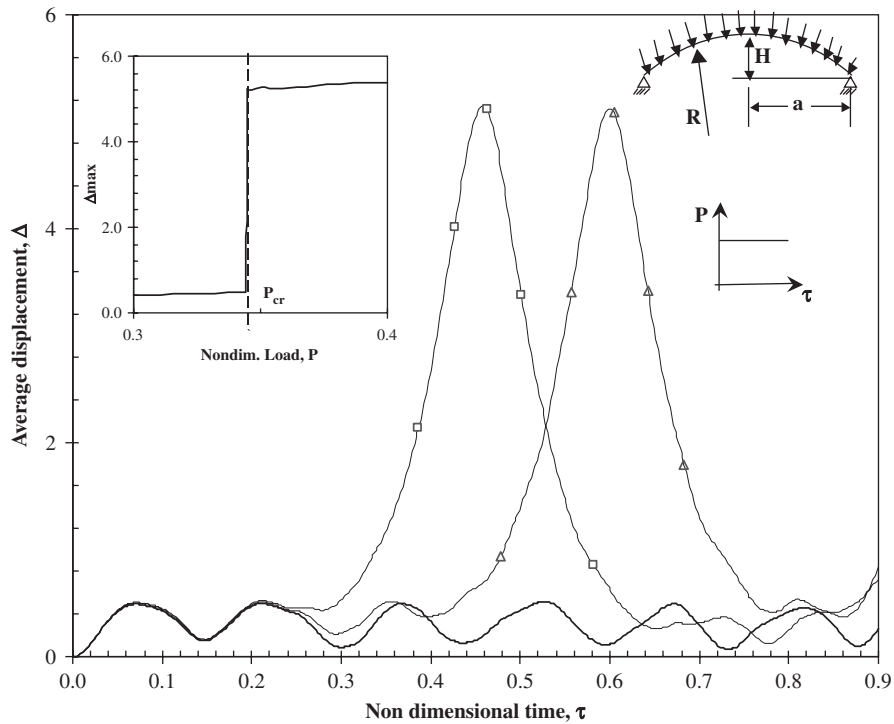


Fig. 3. Average displacement versus non-dimensional time for clamped FGM spherical cap ( $\lambda = 6, k = 1.0$ ):— $P = 0.3$ , —□—  $P = 0.3993$ , —△—  $P = P_{cr} = 0.3449$ .

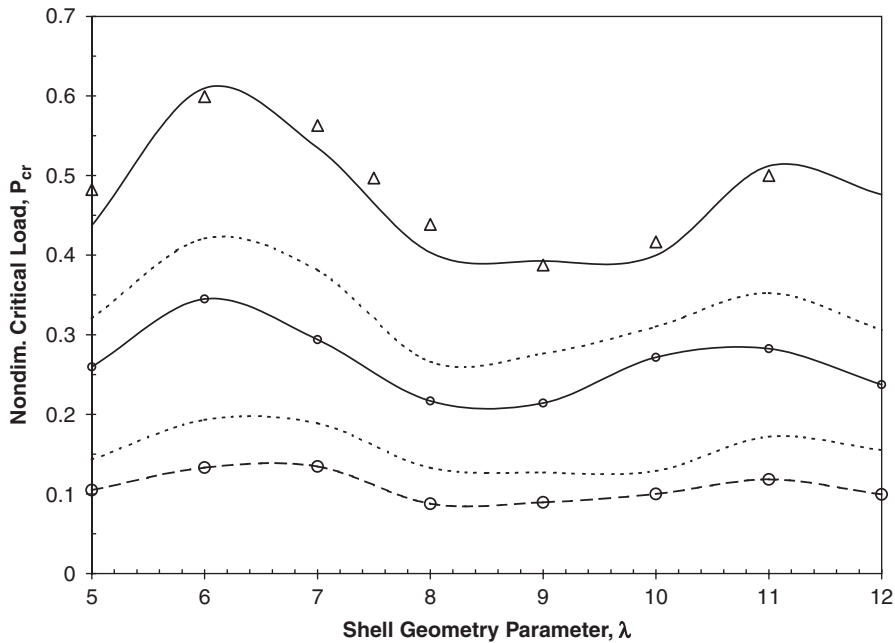


Fig. 4. Variation of non-dimensional critical dynamic pressure against shell geometry parameter ( $\lambda$ ), of clamped FGM spherical cap:  $\Delta$  Huang (isotropic) [3], —  $k = 0.0$  (present-isotropic), - - -  $k = 0.5$ , . . .  $k = 1.0$ , - . - .  $k = 5.0$ , -○- metal.

metallic volumetric fraction and structural coupling due to non-homogeneous nature of FGM. It can be also noted that the rate of decrease in the critical dynamic load value is high with the increase in power law index  $k$  up to 1 and further increase in  $k$  leads to less reduction in  $P_{cr}$ , especially, for very shallow or deep shell cases.



Furthermore, it can be opined that the nature of variation buckling load of FGM shells is qualitatively somewhat similar as those of isotropic case. It is hoped that the present study is useful for the structural engineers while dealing with functionally graded skewed structures.

## References

- [1] B. Budiansky, R.S. Roth, Axisymmetric dynamic buckling of clamped shallow spherical shells, NASA, TND-510, 1962, pp. 597–609.
- [2] G.J. Simitses, Axisymmetric dynamic snap-through buckling of shallow spherical caps, *American Institute of Aeronautics and Astronautics Journal* 5 (1967) 1019–1021.
- [3] N.C. Haung, Axisymmetric dynamic snap-through of elastic clamped shallow shell, *American Institute of Aeronautics and Astronautics Journal* 7 (1969) 215–220.
- [4] W.B. Stephens, R.E. Fulton, Axisymmetric static and dynamic buckling of spherical caps due to centrally distributed pressure, *American Institute of Aeronautics and Astronautics Journal* 7 (1969) 2120–2126.
- [5] R.E. Ball, J.A. Burt, Dynamic buckling of shallow spherical shells., *ASME Journal of Applied Mechanics* 41 (1973) 416–411.
- [6] R. Kao, N. Perrone, Dynamic buckling of axisymmetric spherical caps with initial imperfection, *Computers and Structures* 9 (1978) 463–473.
- [7] J.A. Stricklin, J.E. Martinez, Dynamic buckling of clamped spherical cap under step pressure loadings, *American Institute of Aeronautics and Astronautics Journal* 7 (1969) 1212–1213.
- [8] S. Saigal, T.Y. Yang, R.K. Kapania, Dynamic buckling of imperfection sensitive shell structures, *Journal of Aircraft* 24 (1987) 718–724.
- [9] T.Y. Yang, D.G. Liaw, Elastic-plastic dynamic buckling of thin shell finite elements with asymmetric imperfections, *American Institute of Aeronautics and Astronautics Journal* 25 (1988) 479–485.
- [10] R.S. Alwar, B. Sekhar Reddy, Dynamic buckling of isotropic and orthotropic shallow spherical caps with circular hole, *International Journal of Mechanical Sciences* 21 (1979) 681–688.
- [11] C.C. Chao, I.S. Lin, Static and dynamic snap-through of orthotropic spherical caps, *Composite Structures* 14 (1990) 281–301.
- [12] M. Ganapathi, S.S. Gupta, B.P. Patel, Nonlinear axisymmetric dynamic buckling of laminated angle-ply composite spherical caps, *Composite Structures* 59 (2003) 89–97.
- [13] M. Koizumi, FGM activities in Japan, *Composites* 28 (1997) 1–4.
- [14] A. Makino, N. Araki, H. Kitajima, K. Ohashi, Transient temperature response of functionally gradient material subjected to partial, stepwise heating, *Transactions of the Japan Society of Mechanical Engineering, Part B* 60 (1994) 4200–4206.
- [15] Y. Obata, N. Noda, Steady thermal stresses in a hollow circular cylinder and a hollow sphere of a functionally gradient material, *Journal of Thermal Stresses* 17 (1994) 471–487.
- [16] S. Takezono, K. Tao, E. Inamura, M. Inoue, Thermal stress and deformation in functionally graded material shells of revolution under thermal loading due to fluid, *JSME International Journal Series A: Mechanical and Material Engineering* 39 (1994) 573–581.
- [17] J.F. Durodola, J.E. Adlington, Functionally graded material properties for disks and rotors. In: Proceedings of the First International Conference on Ceramic and Metal Matrix Composites, San Sebastian, Spain, 1996.
- [18] M. Dao, P. Gu, A. Maeqal, R. Asaro, A micro mechanical study of a residual stress in functionally graded materials, *Acta Materialia* 45 (1997) 3265–3276.
- [19] E. Weisenbek, H.E. Pettermann, S. Suresh, Elasto-plastic deformation of compositionally graded metal-ceramic composites, *Acta Materialia* 45 (1997) 3401–3417.
- [20] C. Li, Z. Weng, Z. Duan, Dynamic behavior of a cylindrical crack in a functionally graded interlayer under torsional loading, *International Journal of Solids and Structures* 38 (2001) 7473–7485.
- [21] C. Li, Z. Weng, Z. Duan, Dynamic stress intensity factor of a functionally graded material with a finite crack under anti-plane shear loading, *Acta Mechanica* 149 (2001) 1–10.
- [22] C. Zhang, A. Savais, G. Savais, H. Zhu, Transient dynamic analysis of a cracked functionally graded material by BIEM, *Computers and Material and Science* 26 (2003) 167–174.
- [23] S. Pitakthapanaphong, E.P. Busso, Self-consistent elasto-plastic stress solutions for functionally graded material systems subjected to thermal transients, *Journal of the Mechanics and Physics of Solids* 50 (2002) 695–716.
- [24] C.T. Loy, K.Y. Lam, J.N. Reddy, Vibration of functionally graded cylindrical shells, *International Journal of Mechanical Sciences* 1 (1999) 309–324.
- [25] T.Y. Ng, K.Y. Lam, K.M. Liew, J.N. Reddy, Dynamic stability analysis of functionally graded cylindrical shells under periodic axial loading, *International Journal of Solids and Structures* 38 (2001) 1295–1309.
- [26] G. Prathap, C. Ramesh Babu, A field-consistent three-noded quadratic curved axisymmetric shell element, *International Journal for Numerical Methods in Engineering* 23 (1986) 711–723.
- [27] G.J. Simitses, *Dynamic Stability of Suddenly Loaded Structures*, Springer-Verlag, New York, 1989.
- [28] R.C. Wetherhold, S. Seelman, J. Wang, The use of functionally graded materials to eliminate or control thermal deformation, *Composite Science and Technology* 56 (1996) 1099–1104.
- [29] G.N. Praveen, J.N. Reddy, Nonlinear transient thermoelastic analysis of functionally graded ceramic-metal plates, *International Journal of Solids and Structures* 35 (1998) 4457–4476.
- [30] H. Kraus, *Thin Elastic shells*, Wiley, New York, 1967.

- [31] S. Rajasekaran, D.W. Murray, Incremental finite element matrices, *ASCE Journal of Structures Division* 99 (1973) 2423–2438.
- [32] K. Subbaraj, M.A. Dokainish, A survey of direct time-integration methods in computational structural dynamics II: implicit methods, *Computers and Structures* 32 (1989) 1387–1401.
- [33] P.G. Bergan, R.W. Clough, Convergence criteria for iterative process, *American Institute of Aeronautics and Astronautics Journal* 10 (1972) 1107–1108.
- [34] J.N. Leech, Stability of finite difference equations for the transient response of a flat plate, *American Institute of Aeronautics and Astronautics Journal* 3 (1965) 1772–1773.